Chinese J. Chem. Eng., **14**(6) 734—739 (2006)

Interphase Mass Transfer in G-L-S Magnetically Stabilized Bed with Amorphous Alloy SRNA-4 Catalyst*

LI Wei(李韡)[a], **ZONG Baoning**(宗保宁)[b], **LI Xiaofang**(李晓芳)[a], **MENG Xiangkun**(孟祥坤)[b] **and ZHANG Jinli**(张金利)[a,**]
[a] School of Chemical Engineering, Tianjin University, Tianjin 300072, China
[b] Research Institute of Petroleum Processing, SINOPEC, Beijing 100083, China

Abstract Gas-liquid (G-L) and liquid-solid (L-S) mass transfer coefficients were characterized in a gas-liquid-solid (G-L-S) three-phase magnetically stabilized bed (MSB) using amorphous alloy SRNA-4 as the solid phase. Effects such as superficial liquid velocity, superficial gas velocity, magnetic strength, liquid viscosity, and particle size were investigated. Experimental results indicated that the G-L volumetric mass transfer coefficients (K_La) increased along with the magnetic strength, superficial gas and liquid velocities. Proper increase of liquid viscosity promoted K_La only in the range of lower liquid viscosity. The external magnetic field made L-S mass transfer coefficients (K_s) in the G-L-S MSB lower than those of conventional fluidized beds. K_s in the MSB almost kept constant as the superficial liquid velocity and superficial gas velocity increased and decreased with the liquid viscosity and surface tension, while increased with the particle size K_s showed uniform axial and radial distributions except of small decreases close to the wall. Dimensionless correlations were established to estimate K_La and K_s of the MSB with SRNA-4 catalysts , which showed the average error of 5.4% and 2.5% respectively.
Keywords magnetically stabilized bed, gas-liquid mass transfer, liquid-solid mass transfer, SRNA-4 catalyst

1 INTRODUCTION

Magnetically stabilized beds (MSB) exhibit an unique combination of packed-bed and fluidized-bed properties. Gas-liquid-solid (G-L-S) three-phase MSB has recently attracted more attention in the field of biotechnology processes (such as bioseparation or immobilized enzyme systems) and chemical engineering(such as the hydrogenation reaction system). The interphase mass transfer behavior plays an important role in the optimal operation of practical MSB. However, many reports indicate that both the gas-liquid (G-L) mass transfer coefficients (K_La) and the liquid-solid (L-S) mass transfer coefficient (K_s) are greatly influenced by the operation system in the MSB.

In the case of G-L mass transfer, many investigations studied K_La in the G-L-S MSB with different solid phases. Weng *et al*.[1] reported that the increase of magnetic strength enhanced K_La and established the G-L mass transfer models for three-phase MSB reactors using magnetic alginate particles as the solid. Thompson and Worden[2] studied a three-phase fluidized bed equipped with an axial magnetic field and concluded that K_La maintained the same value or decreases as the magnetic field increased. Al-Qodah and Al-Hassan[3] studied a three-phase stripper containing magnetic Fe_3O_4 particles under the external radial magnetic field and claimed that K_La become higher as the gas velocity and the magnetic strength increased, and K_La showed a linear relationship with the gas velocity at a constant magnetic strength. Chen and Leu[4] investigated the mass transfer of three-phase MSB with Ni powders of 194μm diameter and concluded that K_La of MSB was enhanced by the magnetic strength and could be increased by 70％ at higher magnetic strength, which was close to the mass transfer coefficient of G-L bubbled columns.

On the other hand, there were only few reports with controversial conclusions on the local L-S mass transfer behavior in the G-L-S MSB. Some investigations[5—8] suggested that the external magnetic force enhanced the L-S mass transfer, and K_s increased with the magnetic strength. However, other reports[9—11] indicated that the external magnetic field played negative roles in K_s.

The ferromagnetic catalyst of SRNA-4, an amorphous nickel alloy catalyst, has high hydrogenation activity at low temperature. Meng *et al*.[12] has used SRNA-4 in the MSB for purification of caprolactam. So far, no report has been found about the interphase mass transfer characteristic of the G-L-S MSB with commercial magnetic catalyst particles of SRNA-4. In this study, K_La and K_s in the G-L-S MSB using amorphous alloy SRNA-4 as the magnetic solid phase are measured and correlated. The results may be valuable to the practical design and optimization of MSB using SRNA-4 as the catalyst.

2 EXPERIMENTAL

A schematic diagram of the experimental appa-

Received 2005-11-08, accepted 2006-02-26.
* Supported by the National Natural Science Foundation of China (No.20206023, No.20676096), the Special Funds for Major State Basic Research Program of China (973 Program, 2006CB202500), and SINOPEC (X504029).
** To whom correspondence should be addressed. E-mail: zhangjinli@tju.edu.cn

ratus of a magnetically stabilized bed is shown in Fig.1. The Plexiglas column is 1.5m in height with an i.d. of 0.1m. The axially uniform magnetic field was provided by seven similar DC-powered copper wire coils surrounding the column with 0.16m i.d. and 0.1m in height. All experiments were carried out at (25±1)℃. The liquid flow rate was measured by calibrated rotameters with the precision of 2.5%. As the gas phase, air was introduced into the reactor through an air compressor, the air volumetric flow rate was measured by the rotameter (with the precision of 2.5%). The solid phase was spherical amorphous alloy catalyst SRNA-4[12] with the diameter of 80—120μm and 120—200μm, the apparent density of 2500kg·m^{-3}. The viscosity of the solution was adjusted within the range of 1—5mPa·s by the adding of sodium carboxymethyl cellulose and measured by a viscometer (NDJ-7, Shanghai Tianping). Surface tension of solutions was adapted to the range of 54—72mN·m^{-1} by the addition of a nonionic surfactant and measured by a tensiometer (XP-2000, ZhongChen).

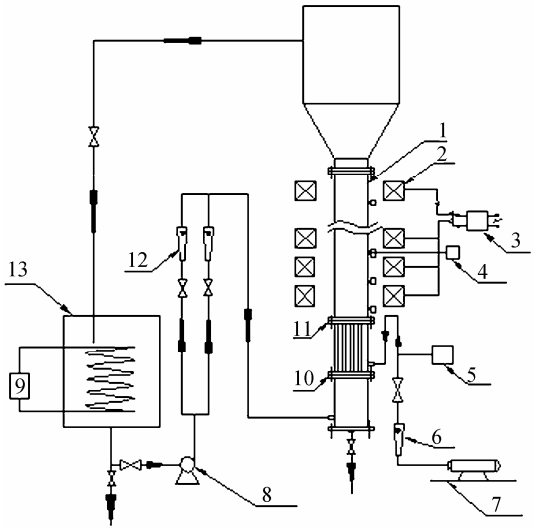

Figure 1 Experimental set-up of MSB
1—fluidized bed; 2—field coils; 3—direct power; 4—testing instrument; 5—pressure sensor; 6—gas rotameter; 7—air compressor; 8—liquid pump; 9—heater and controller; 10—liquid distributor; 11—gas-liquid distributor; 12—liquid rotameter; 13—liquid tank

Sodium sulfite (0.5mol·L^{-1}) aqueous solution was used as the liquid phase, which contained 0.001mol·L^{-1} cobalt sulfate as the catalyst for the oxidation of sulfite. The overall G-L volumetric mass transfer coefficient, K_La, is determined by means of the oxidation of sodium sulfite method[13]. Oxygen concentration of the gas phase and sodium sulfite concentration of the liquid phase inside the reactor was measured using the titrimetry.

The electrolytic solution was a mixture of 0.001mol·L^{-1} potassium ferrocyanide, 0.001mol·L^{-1} potassium ferricyanide and 0.02mol·L^{-1} sodium hydroxide. Sodium hydroxide was added as the electrolyte support to minimize the migration effects. The electrochemical method[14—16] was used to measure the local L-S mass transfer coefficients(K_s) in the MSB.

3 RESULTS AND DISCUSSION

3.1 G-L mass transfer behavior

3.1.1 *Effects of the magnetic strength on K_La*

Figure 2 indicated that K_La increased with the magnetic strength within the experimental range. The average gas holdup was proportional to the magnetic strength, *i.e*, the higher magnetic strength, the larger average gas holdup ε_g (Fig.3). Additionally, it was observed that the size of air bubbles decreased obviously as the magnetic strength increased, which enhanced the interfacial area as well as K_La.

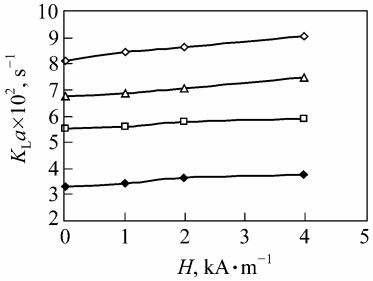

Figure 2 Effect of magnetic strength on K_La
(μ=1mPa·s, d_p=80—120μm, U_l=1.13mm·s^{-1})
U_g, mm·s^{-1}: ◆ 1.77; □ 2.83; △ 3.54; ◇ 4.25

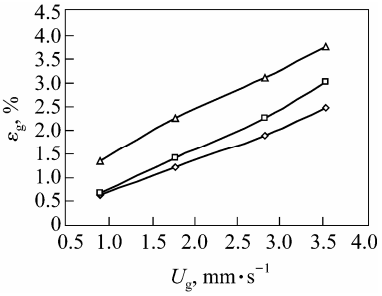

Figure 3 Average gas holdup as a function of magnetic strength and gas velocity
(μ=1mPa·s, d_p=80—120μm, U_l=1.42mm·s^{-1})
H, kA·m^{-1}: ◇ 0; □ 1; △ 2

3.1.2 *Effects of superficial gas velocity on K_La*

Figure 4 showed the effects of gas velocity on K_La, which indicated approximately linear relationship between K_La and the gas velocity within the experimental range of magnetic strength and liquid velocity. It is reasonable because the average gas holdup increases and the average size of air bubbles decreases with the increase of gas velocity, which enhance the interface areas between gas and liquid phase. On the other hand, the higher gas velocity accelerates the rising rate of air bubbles in the bed and promotes the liquid turbulences around air bubbles, which reduce the mass transfer resistance between the liquid film around the bubble surface and the bulky liquid phase, and consequently made K_La increased.

3.1.3 *Effects of superficial liquid velocity on K_La*

Figure 5 showed that K_La increased only slightly

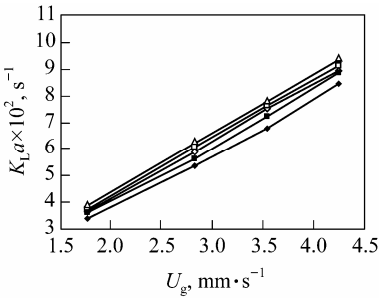

Figure 4 Effect of superficial gas velocity on K_La
(μ=1mPa·s, d_p=80—120μm)
◆ H=0, U_l=1.13mm·s^{-1}; ■ H=2kA·m^{-1}, U_l=1.13mm·s^{-1}; ▲ H=4kA·m^{-1}, U_l=1.13mm·s^{-1}; ◇ H=0, U_l=1.42mm·s^{-1}; □ H=2kA·m^{-1}, U_l=1.42mm·s^{-1}; △ H=4kA·m^{-1}, U_l=1.42mm·s^{-1}

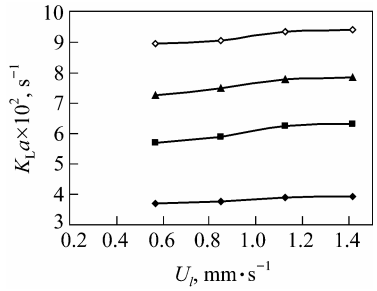

Figure 5 Effect of superficial liquid velocity on K_La
(μ=1mPa·s, d_p=80—120μm, H=4kA·m^{-1})
U_g, mm·s^{-1}: ◆ 1.77; ■ 2.83; ▲ 3.54; ◇ 4.25

with the liquid velocity. According to the assumption of Lara-Marquez *et al*.[17], the average diameter of air bubbles is in proportion to turbulent micro-scales. Therefore, the G-L interfacial area increased in strongly turbulent liquid phase and then K_La become larger.

3.1.4 *Effects of liquid viscosity on K_La*

The higher liquid viscosity facilitated both the increase of air bubble size and the average gas holdup (as shown in Fig.6). These two factors have adverse influences on the G-L interfacial areas. Fig.6 indicated that the average gas holdup has significant effects on the G-L interfacial areas, comparing with those on the average size of air bubbles. Thus, K_La increased with the liquid viscosity in our experimental range (μ<5mPa·s) (as shown in Fig.7). This is consistent with Chen and Leu[18] who reported that the K_La value increased at lower liquid viscosity (μ<5mPa·s) while decreased at higher liquid viscosity (μ>5mPa·s) using gas distributors with small pore diameter (0.1mm).

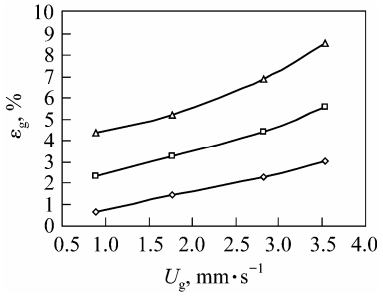

Figure 6 Effect of liquid viscosity on average gas holdup
(d_p=80—120μm, H=1kA·m^{-1}, U_l=1.42mm·s^{-1})
μ, mPa·s: ◇ 1; □ 3; △ 5

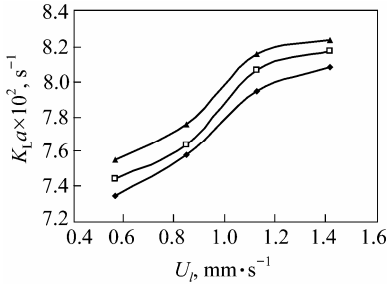

Figure 7 Effect of liquid viscosity on K_La
(d_p=80—120μm, U_g=3.54mm·s^{-1}, H=4kA·m^{-1})
μ, mPa·s: ◆ 1; □ 3; ▲ 5

3.2 L-S mass transfer behavior

3.2.1 *Effect of superficial liquid velocity and magnetic strength on K_s*

Figure 8 indicated that K_s almost kept unchanged with the liquid velocity. Song[19] draw the consistent conclusion in a convention G-L-S three-phase fluidized beds by using benzoic acid miscibility to measure K_s. As the magnetic strength increased, K_s in the MSB decreased, which is attributed to the influence of the magnetic field on the particle coalescence. Under higher magnetic strength, singly particles in the fluidized bed gradually transferred into double-, triplet-, or even multi-particle clusters. Consequently the L-S mass transfer resistance became larger and the swaying velocity of solid particles was limited, which resulted in the lower value of K_s .

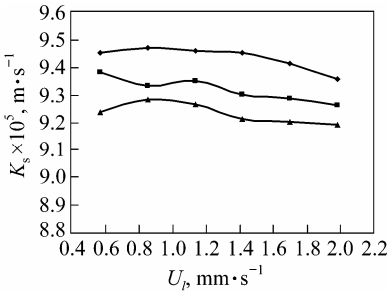

Figure 8 Effect of liquid superficial velocity and magnetic field intensity on K_s
(μ=1mPa·s, σ=71.97mN·m^{-1}, U_g=1.77m·s^{-1}, d_p=80—120μm)
H, kA·m^{-1}: ◆ 0; ■ 2; ▲ 4

3.2.2 *Effect of superficial gas velocity on K_s*

K_s slightly increased with the lower superficial gas velocity, then turned to be constant at higher gas velocity (as shown in Fig.9). At the initial stage of introducing air into the bed, the liquid turbulence is accelerated, however, the full-developed turbulence of the bulky liquid will not obviously change even at higher superficial gas velocity, which resulted in approximately constant value of K_s at higher gas velocity.

3.2.3 *Effect of liquid viscosity on K_s*

Figure 10 indicated that K_s decreased with the increase of liquid viscosity. As the liquid viscosity increased, the diffusion coefficient become smaller and the diffusion boundary layer become thicker, which made K_s decreased at higher liquid viscosity.

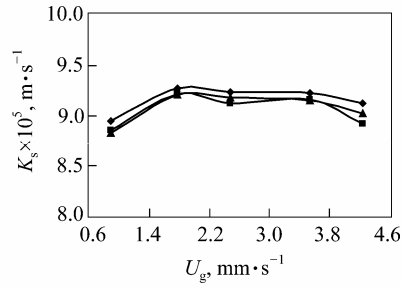

Figure 9 Effects of gas superficial velocity on K_s
(μ=1mPa·s, H=4kA·m^{-1}, d_p=80—120μm, σ=71.97mN·m^{-1})
U_l, m·s^{-1}: ◆ 1.33; ■ 1.42; ▲ 1.70

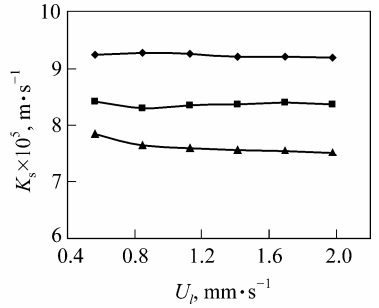

Figure 10 Effect of liquid viscosity on K_s
(σ=71.97mN·m^{-1}, H=4Ka·m^{-1}, d_p=80—120μm, U_g=1.77m·s^{-1})
μ, mPa·s: ◆ 1; ■ 3; ▲ 5

3.2.4 *Effect of liquid surface tension on K_s*

As the liquid surface tension decreased, K_s become larger (Fig.11). The lower liquid surface tension can prevent the air bubbles from coalescence but enhance the gas holdup, so that there appeared much more small air bubbles and the surface renewal frequency was faster than that under higher surface tension. Thus the L-S mass transfer coefficient increased which is accordance to the diffusion theory of Surface Renewal Model.

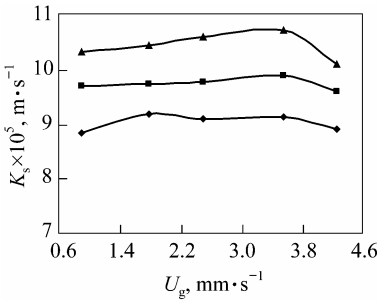

Figure 11 Effect of liquid surface tension on K_s
(μ=1mPa·s, σ=71.97mN·m^{-1}, H=4kA·m^{-1}, d_p=80—120μm, U_l=1.42m·s^{-1})
σ, mN·m^{-1}: ◆ 71.97; ■ 61.44; ▲ 54.42

3.2.5 *Effect of particle size on K_s*

Figure 12 indicated that K_s with larger particles was higher than that with smaller size particles. In the case of larger particles, the liquid turbulence is stronger than that of smaller particles, which leads to the decrease of the diffusion boundary layer. It is the decreased diffusion boundary layer that results in the higher K_s with larger particles.

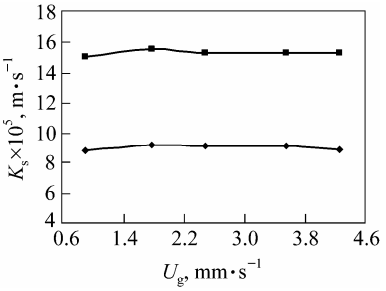

Figure 12 Effect of particle size on K_s
(μ=1mPa·s, σ=71.97mN·m^{-1}, H=4kA·m^{-1}, U_l=1.42mm·s^{-1})
d_p, μm: ◆ 80—120; ■ 120—200

3.2.6 *Radial and axial distributions of K_s*

K_s showed similar tendency of its radial distribution under various operating and property parameters. Close to the wall occurred small decrease of K_s, whereas no variation of K_s was observed along other radial positions (as shown in Fig.13). Fig.14 indicated that K_s had a uniform axial distribution in the G-L-S three-phase MSB.

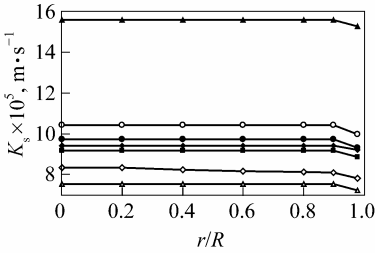

Figure 13 Radial distributions of K_s
◆ H=0, μ=1mPa·s, d_p=80—120μm, σ=71.97mN·m^{-1};
■ H=4kA·m^{-1}, μ=1mPa·s, d_p=80—120μm, σ=71.97mN·m^{-1};
● H=4kA·m^{-1}, μ=1mPa·s, d_p=80—120μm, σ=61.44mN·m^{-1};
○ H=4kA·m^{-1}, μ=1mPa·s, d_p=80—120μm, σ=54.42mN·m^{-1};
◇ H=4kA·m^{-1}, μ=3mPa·s, d_p=80—120μm, σ=71.97mN·m^{-1};
△ H=4kA·m^{-1}, μ=5mPa·s, d_p=80—120μm, σ=71.97mN·m^{-1};
▲ H=4kA·m^{-1}, μ=1mPa·s, d_p=120—200μm, σ=71.97mN·m^{-1}

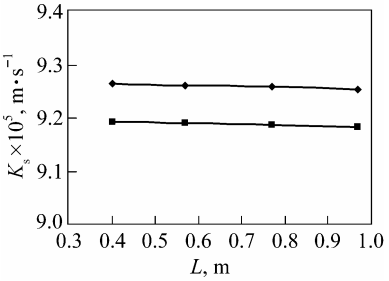

Figure 14 Axial distributions of K_s
(μ=1mPa·s, σ=71.97mN·m^{-1}, d_p=80—120μm, U_l=1.77mm·s^{-1}, U_g=1.98mm·s^{-1})
H, kA·m^{-1}: ◆ 2; ■ 4

3.3 Correlations for G-L and L-S mass transfer coefficients

Based on the experimental results, it is suggested that the G-L volumetric mass transfer coefficient is the function of magnetic strength, gas and liquid velocity and liquid viscosity in the MSB. The following dimensionless correlation was developed to estimate K_La in this type of MSB.

$$Sh_1 = 1.46 Re_1^{0.0813} Fr_1^{0.491} Sc^{1.05} Ga^{0.478} \exp(0.183 H / H_{max}) \quad (1)$$

Eq.(1) fits the experimental data well under the measured conditions, *i.e.*, the particle diameter of 80—120μm, H=0—8kA·m^{-1}, U_g=0.6—4.2mm·s^{-1}, U_l=1.2—2.6mm·s^{-1}, and μ=1—5mPa·s. The average error between the calculated and the experimental data is 5.4%.

Combining the effect of magnetic strength with the method of Hassanien[20] for L-S mass transfer coefficients, the correlated equation was obtained as below to estimate K_s.

$$Sh_2 = 0.472 Fr_2^{0.00443} Ga^{0.420} Re_2^{-0.0141} Sc^{1/3} \exp(-0.0802 H / H_{max}) \quad (2)$$

Eq.(2) fits the experimental data well under the measured conditions, *i.e.*, the particle diameter of 80—200μm, H=0—8kA·m^{-1}, U_g=0.6—4.2mm·s^{-1}, U_l=1.2—2.6mm·s^{-1}, μ=1—5mPa·s, and σ=54—72mN·m^{-1}. The average error between the calculated and the experimental data is 2.5%.

4 CONCLUSIONS

Both G-L and L-S mass transfer behavior in G-L-S magnetically stabilized bed were studied under various conditions using amorphous alloy catalysts SRNA-4 as the solid phase. Experimental results indicated that the external magnetic field provided higher G-L volumetric mass transfer coefficients in three-phase MSB, comparing with those in conventional G-L-S fluidized beds. K_La increased along with the magnetic strength, superficial gas and liquid velocities, besides liquid viscosity with lower values. A correlated equation was established to estimate K_La of the MSB, and the average error between the estimated and the experimental data was 5.4%.

It was found that L-S mass transfer coefficients in the G-L-S MSB using amorphous alloy catalysts SRNA-4 were lower than those in conventional fluidized beds. K_s almost kept constant as the superficial liquid velocity and superficial gas velocity increased, whereas decreased with the liquid viscosity and surface tension. However, K_s increased with the particle size of SRNA-4 catalyst. K_s showed uniform axial and radial distributions except of slight decrease close to the wall. A correlated equation of K_s was established in the MSB, and the average estimation error was 2.5%.

NOMENCLATURE

D	diffusion coefficient, m^2·s^{-1}
D_c	diameter of reactor, m
d_p	diameter of particle, m
Fr_1	Froude number ($Fr=U_g^2/gD_c$)
Fr_2	Froude number of the solid phase ($Fr=U_g^2/gd_p$)
Ga	Galileo number ($Ga=d_p^3 g\rho^2/\mu^2$)
g	standard gravity acceleration, m·s^{-2}
H	magnetic field intensity, kA·m^{-1}
H_{max}	max magnetic field intensity(H_{max}=8 kA·m^{-1})
K_La	gas-liquid mass transfer coefficient, s^{-1}
K_s	liquid-solid mass transfer coefficient, m·s^{-1}
Re_1	Reynolds number for liquid ($Re=D_cU_l\rho_l/\mu_l$)
Re_2	Reynolds number for liquid ($Re=(U_l d_p \rho/\mu)$
Sc	Schmidt number of the solutions ($Sc=\mu/\rho D$)
Sh_1	Sherwood number of the solutions ($Sh=K_La\cdot D_c^2/D$)
Sh_2	Sherwood number of the solutions ($Sh=K_sd_p/D$)
U_g	superficial gas velocity, mm·s^{-1}
U_l	liquid superficial velocity, mm·s^{-1}
ε_g	gas holdup, %
μ	liquid viscosity, mPa·s
ρ	density, kg·m^{-3}
σ	liquid surface tension, mN·m^{-1}

REFERENCES

1 Weng, D.C., Cheng, L.N., Han, Y., Zhu, W.X., Xu S.M., Ouyang, F., **"**Continuous ethanol fermentation in a three-phase magnetic fluidized bed bioreactor", *AIChE Symposium Series, Fluidized Processes: Theory and Practice*, **88**, 107—115(1992).

2 Thompson, V.S, Worden, R.M, "Phase holdup, liquid dispersion, and gas-to-liquid mass transfer measurements in a three-phase magnetofluidized bed", *Chem. Eng. Sci.*, **52**, 279—295(1997).

3 Al-Qodah, Z., Al-Hassan, M., "Phase holdup and gas-to-liquid mass transfer coefficient in magneto stabilized G-L-S airlift fermenter", *Chem. Eng. J.*, **79**, 41—52(2000).

4 Chen, C.M., Leu, L.P., "Hydrodynamics and mass transfer in three-phase magnetic fluidized beds", *Powder Technol.*, **117**, 198—206(2001).

5 Webb, C., Kang, H.K., Moffat, G., Williams, R.A., **"**Magnetically stabilized fluidized bed bioreactor: A tool for improved mass transfer in immobilized enzyme systems", *Chem. Eng. Biochem. Eng.*, **61**, 241—246(1996).

6 Jovanovic, G., Al-Mulhim M., "Liquid-solid mass transfer in magnetically stabilized fluidized beds", In: A.I.Ch.E. Annual Meeting, Miami Beach, CA (1995).

7 Bramble, J.L., Graves, D.J., Brodelius, P., "Plant cell culture using a novel bioreactor: The magnetically stabilized fluidized bed", *Biotechnol. Prog.*, **6**, 452—457(1990).

8 Hausmann, R., Reichert, C., Franzreb, M., Holl, W. H., "Liquid-phase mass transfer of magnetic ion exchangers in magnetically fluidized beds II. AC field", *React. Funct. Polym.*, **60**, 17—26(2004).

9 Hausmann, R., Hoffmann, C., Franzreb, M., Holl, W.H., "Mass transfer rates in a liquid magnetically stabilized fluidized bed of magnetic ion-exchange particles", *Chem. Eng. Sci.*, **55**, 1477—1482(2000).

10 Franzreb, M., Hausmann, R., Hoffmann, C., Holl, W.H., "Liquid-phase mass transfer of magnetic ion exchangers in magnetically fluidized beds I. DC fields", *React. Funct. Polym.*, **46**, 247—257(2001).

11 Cheng, C.Y., Yung, K., "Effect of magnetic field on heat and mass transfer by natural convection from vertical surfaces in porous media-an integral approach", *Int. Comm. Heat Mass Transfer*, **126**, 935—943(1999).

12 Meng, X.K., Mu, X.H., Zong, B.N., Min, E.Z., Zhu, Z.H., Fu, S.B., Luo, Y.B.. "Purification of caprolactam in magnetically stabilized bed reactor", *Catal. Today*, 79—80, 21—27(2003).

13 Zhang, Y.Q., Mao, Z.S., Chen, J.Y., "Gas-liquid mass transfer of oxygen-decane-sodium sulfite system in a

stirred autoclave reactor", *Eng. Chem. Metall*, **21**,123—127(2000). (in Chinese)
14 Rao, V.G, Drinkenburg, A.A.H, "Solid-liquid mass transfer in packed beds with cocurrent gas-liquid downflow", *AIChE J.*, **31**, 1059—1068(1985).
15 Yasunishi, A., Fukuma, M., Muroyama, K., "Wall-to-liquid mass transfer in packed and fluidized beds with gas-liquid concurrent upflow", *J. Chem. Eng. Jpn.* **21**, 522—528(1988).
16 Muroyama, K., Yoshikawa, T., Takakura, S., Yamanaka, Y., "Mass transfer from an immersed cylinder in three-phase systems with fine suspended particles", *Chem. Eng. Sci*., **52**, 3861—3868(1997).
17 Lara-Marquez, A., Larachi, F., Wild, G., Laurent, A., "Mass transfer characteristics of fixed beds with concurrent upflow and downflow, A special reference to the effect of pressure", *Chem. Eng. Sci*., **47**, 3485—3492(1992).
18 Chen, C.M., Leu, L.P., "A highly elevated mass transfer rate process for three-phase liquid-continuous fluidized beds", *Chem. Eng. J*., **81**, 223—230(2001).
19 Song, J., Hyndman, C. L, Kantzas, A, "Effect of particle tethering and scale-up on solid-liquid mass transfer in three-phase fluidized beds of light particles", *Can. J. Chem. Eng*., **79**, 557—563(2001).
20 Hassanien, D.S.H, Riba, J.L., "Transfer de matiere liquide-particules en fluidisation a trios phase", *Entropie*, **119**, 17—26(1984).